



Research Paper

Electrical Properties of Nickel Nanowires Modified by 2.75 MeV Proton Ions

Shehla Honey^{a, d, e, *}, Jamil Asim^{b, c}, Adnan S Khan^c, Maaza M.^{d, e}

^aCentre for Nanosciences, University of Okara, Okara, Pakistan

^bUniversity of Okara, Okara Pakistan

^cFaculty of Computer Science and Information Technology, Universiti Malaysia Sarawak, Malaysia

^dUNESCO-UNISA Africa Chair in Nanosciences/Nanotechnology, College of Graduate Studies, University of South Africa, Muckleneuk ridge, P O Box 392, Pretoria, South Africa,

^eNanosciences African Network (NANOAFNET), iThemba LABS, National Research Foundation, Old Faure road, P O Box 722, Somerset West 7129, South Africa

ABSTRACT

Electrical conductivity of Nickel Nanowires (Ni-NWs) was reported in this work. The Ni-NWs was irradiated with 2.75 MeV proton (H^+) ions at various fluencies of H^+ ions ranging from 5×10^{14} to $\sim 1 \times 10^{16}$ ions/cm². The electrical conductivity of formulated Ni-NWs networks was observed to decrease as the H^+ ions beam fluencies reduces. This may be adduced to the buildup of clusters of defects in materials. With the increase of beam fluencies, the electrical conductivity increases and this may be attributed to a reduction in wire-wire point contact resistance relatively to the irradiation-induced coalescence. Coalescence is probably initiated due to H^+ ions-irradiation induced heating effect that improved the crystalline quality of nanowires (NWs). The fabricated Ni-NWs networks subjected to an ion beam irradiation to observe corresponding changes in electrical conductivity; are promising for application as highly transparent and conducting electrodes.

KEYWORDS: Ni-Nanowires, H^+ ions irradiation, Nano-welding, Electrical conductivity.

Received 08 December, 2020; Accepted 24 December, 2020 © The author(s) 2020.

Published with open access at www.questjournals.org

I. INTRODUCTION

For streaming of charge carriers in many new technologies, strongly conductive networks of metal nanowires (MNWs) are essential [1]. In 2008, after the observation of P. Peumans et al. [2] it was revealed that MNWs mesh based transparent electrodes appeared to be leading contenders in the industry of transparent electrodes. According to estimation of nano-market, revenue from MNWs based transparent electrodes will surpass \$255 million. A good percolation path is offered by MNWs networks to the surge of charge carriers which is credited to intrinsic metallic nature of MNWs. In MNWs networks, nanowire-nanowire junction point is the main resistance point which needs to be welded or well-connected [3]. For NW-NW junction points welding, several techniques have been reported by researchers such as: cold welding [4], pulse laser processing [5], Joule heat welding [6], [2, 7]. Besides, welding by exposing nanomaterials to energetic ions is an important tool for nanowire-nanowire junction. This technique is applicable to variety of nanomaterials [8-14]. A general conception about exposure of nanomaterials to energetic ions is explosion of structure of materials but the other positive aspect is to tailor the electronic, structural, optical and magnetic [15, 8, 9, 16] properties of nanomaterials [11]. In one of previous report, Bari et al reported the electrical conductivity of Ag-NWs networks has been increased through ion beam irradiation technology. Similarly, in another report, we found enhancement in conductivity of Ag-NWs [14] networks by MeV H^+ ions. After Ag-NWs, we tried to implement

this technique to modify conductivity of other types of metallic NWs. Firstly; we prepared the drop casted networks of Ni-NWs and irradiated these samples with a beam of 2.75MeV H⁺ ions to obtain welds between NWs. Drop casting is found to be an economical and simple technique to provide uniformly distributed NWs networks which then can be followed with ion beam irradiation for welding at contact points.

II. EXPERIMENTAL SECTION

Nickel nanowires (Product ID: PL-NiW200) was obtained from PlasmaChem GmbH with \approx 300-500nm diameter and \approx 100-200 μ m length. The wool-like fibers Ni-NWs was converted into an aqueous solution. The aqueous solution was prepared using 5mg of Ni-NWs fiber in 1mL of ethanol. The Solution of Ni-NWs was deposited on a substrate made of glass via drop casting technique. The schematic representation of experiment can be seen in Figure 1.

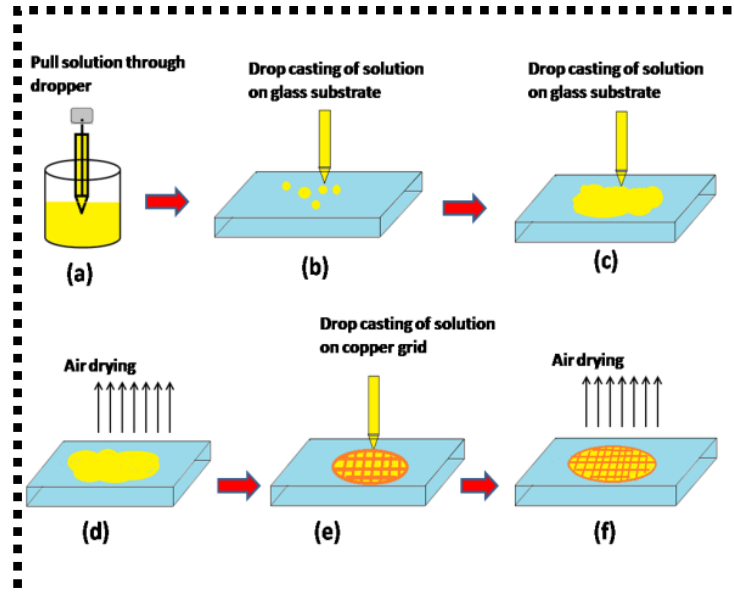


Figure 1: Various experimental steps of drop casting of solution on glass substrate.

The samples were thereafter subjected to ion beam irradiation of 2.75 MeV at room temperature (R_T) with varying fluencies ranging from 5×10^{14} to 1×10^{16} ions/cm² using a 5UDH-Pelletron accelerator at $\sim 10^{-7}$ Pa. The Stopping Range of Ions in Matter (SRIM) simulation was done to obtain information about implantation of H⁺ ions into Ni-NWs during irradiation. The structural and morphological analysis of Ni-NWs was characterized using transmission electron microscopy (TEM) and X-ray diffraction (XRD) techniques. Electrical conductivity measurement was conducted using four probe and four-point probe techniques respectively. The voltage potential “V” in the probe is measured using the expression in equation 1 [14].

$$V = 1/2\pi SG \quad (1)$$

Where G is “surface conductivity” and Si is “distance of current and voltage probes” and I is “current”.

III. RESULTS AND DISCUSSIONS

The pristine arbitrarily arranged Ni-NWs deposited on the glass substrate is shown in Figure 2 (a). These networks show that NWs are self-assembled by Vander Waals forces with NWs density well above the percolation threshold. The diameters of pristine Ni-NWs ranges between 300-500nm (see Figure 2 (a)). These Ni-NWs have polycrystalline nature and it is verified from HRTEM image of Figure 2(b) which is further confirmed through SAED image of Figure 2 (c). EDX spectra of un-irradiated Ni-NWs (Figure 2 (d)) shows trace elements of Ni and Cu. Ni is the main trace element and Cu might be appeared due to copper grids that employed during TEM analysis of un-irradiated sample. For TEM analysis, solution of Ni-NWs was drop casted on copper grids. After irradiation of Ni-NWs with a fluence of 5×10^{14} ions/cm², coalescence or joining was not observed as shown in Figure 2 (e). Morphology of NWs is also preserved.

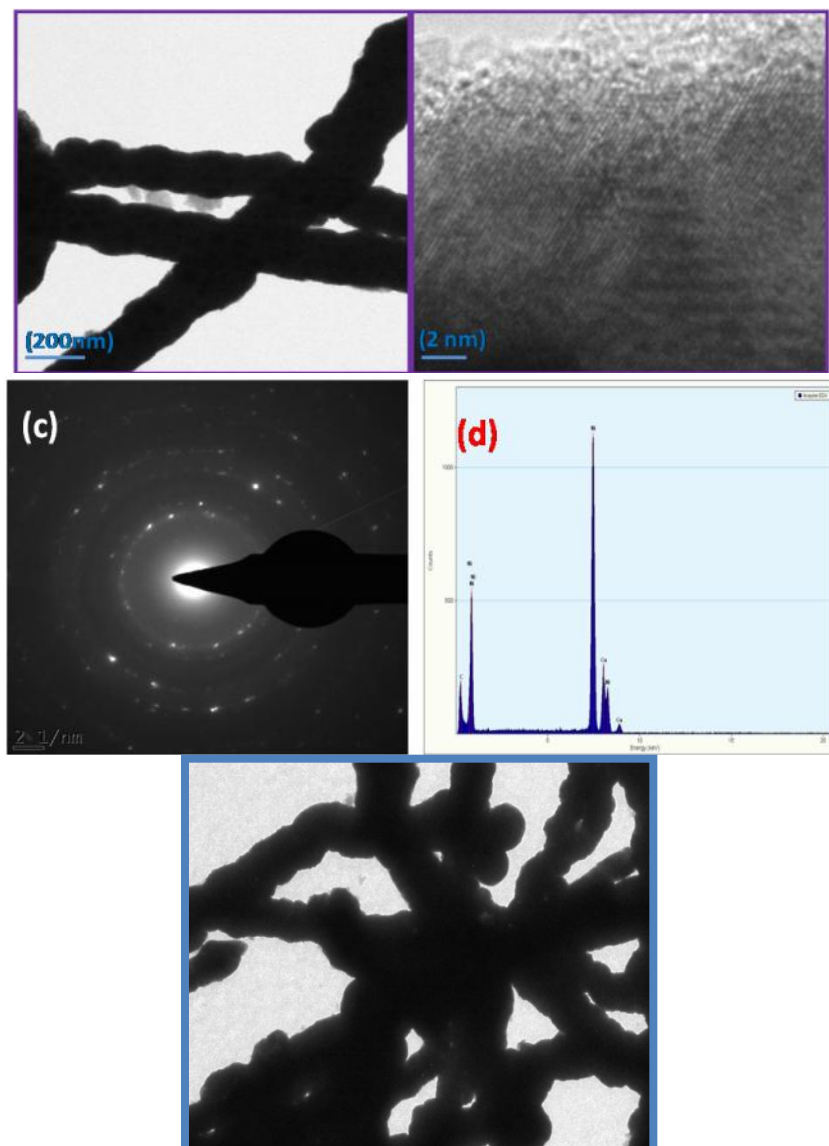


Figure 2: (a) Un-irradiated Ni-NWs (b) HRTEM of Ni-NWs (c) SAED image of un-irradiated Ni-NWs (d) EDX spectra (e) Ni-NWs network irradiated by H^+ ions (2.75 MeV) at a fluence 5×10^{14} ions/cm²

The Ni-NWs start to coalesce or joined with each other after irradiation at $\sim 5 \times 10^{15}$ ions/cm² fluence as seen in Figure 3. The reason for coalescence of these NWs is due to ion irradiation-induced heating effect. The formation of junctions of Ni-NWs in various shapes such as cross and parallel shapes is initiated and can be clearly seen in Figure 3 due to H^+ ion irradiation-induced coalescence that might lead to form welded network of Ni-NWs. Furthermore, it can also be seen in HRTEM images of Figure 3 that morphology of NWs is still preserved. The clear preview of un-welded parts can also be seen in Figure 3 (b); however welded NWs at this dose are also highlighted in Figure 3 (c).

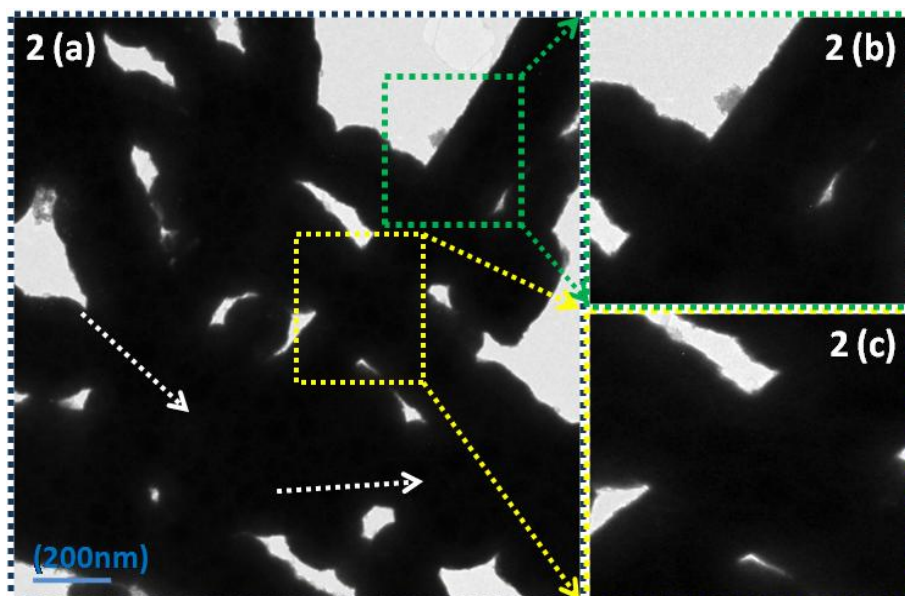


Figure 3: Ni-NWs network irradiated by 2.75 MeV H^+ ions at fluence 5×10^{15} ions/cm²

With the increase of beam fluence up to $\sim 1 \times 10^{16}$ ions/cm², a clear NWs network formation was observed. The TEM images of the junctions that have been fused/welded due to ion beam irradiation are presented in Figure 4. Also, the corresponding HRTEM images of welded cross and parallel junctions were presented in Figure 4. It is clear from Figure 4 that the morphology of Ni-NWs is still preserved at $\sim 1 \times 10^{16}$ ions/cm² fluence; hence, eliminating sputtering after the irradiation of samples at ion beam fluence of $\sim 1 \times 10^{16}$ ions/cm². Moreover, it is also seen in Figure 4 that NWs are perfectly welded to each other.

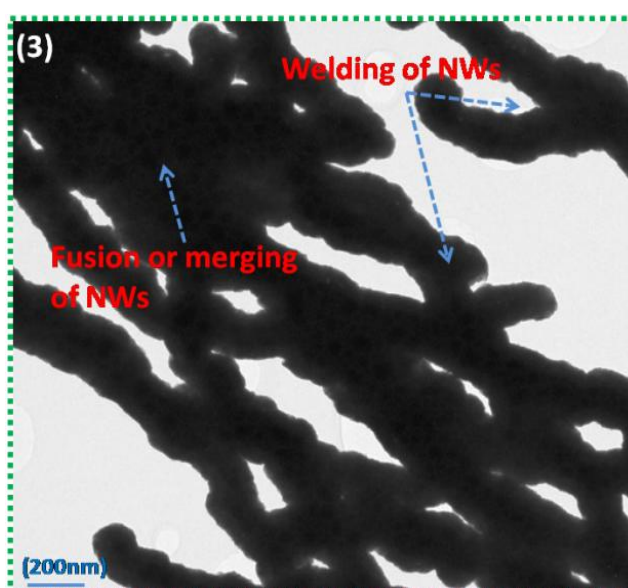


Figure 4: Ni-NWs network irradiated by 2.75 MeV H^+ ions at fluence 1×10^{16} ions/cm²

The clear preview of welded parts of Figure 4 is seen in Figure 5 (a-c). Figure 5 (a-c) shows NWs are well-connected to each other in Y-, X- and II-shapes.

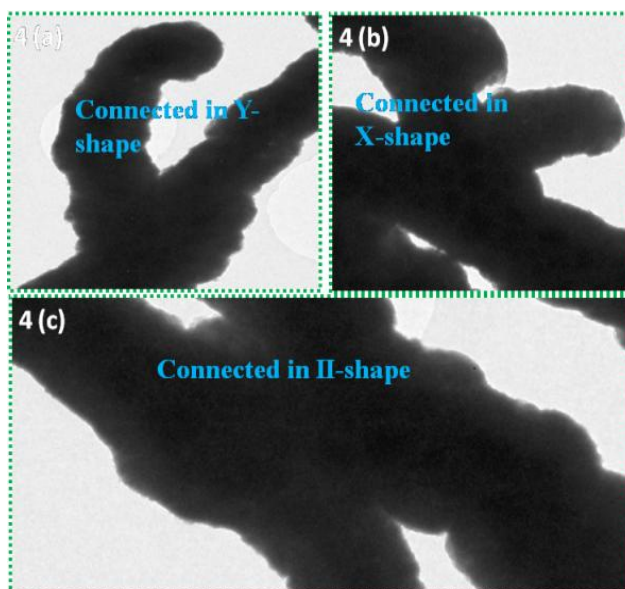


Figure 5: Ni-NWs network irradiated by 2.75 MeV H^+ ions at fluence 1×10^{16} ions/cm² (a-c) shows NWs connected in Y-, X- and II-shapes.

As the ions beam fluence increases to $\sim 5 \times 10^{17}$ ions/cm², NWs started to melt, fuse and lose the actual shape leading to irrecoverable damage as shown in the TEM images of Figure 6.

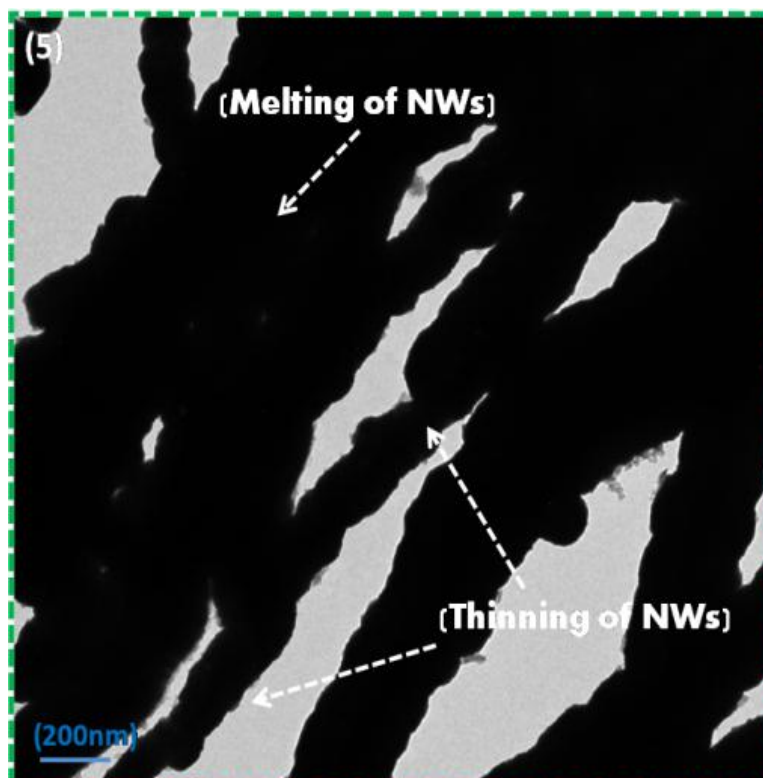


Figure 6: Ni-NWs network irradiated by H^+ ions (2.75 MeV) at fluence 5×10^{17} ions/cm² shows thinning and melting of NWs.

Surplus or high ions beam fluencies were avoided due to keep safe from damaging effect in NWs due to excessive power of ions. Similarly, in case of low beam fluencies, less number of defects or less heat would be generated; this is insufficient to effectively connect NWs on overlapping positions. Therefore, medium doses and ions beam energies were selected to achieve optimized results [17]. After examining the Ni-NWs networks by TEM, the structural evaluation of Ni-NWs network before and after irradiation with 2.75 MeV H^+ ions is also important. Structural evaluation was made to observe changes in crystalline structure of NWs.

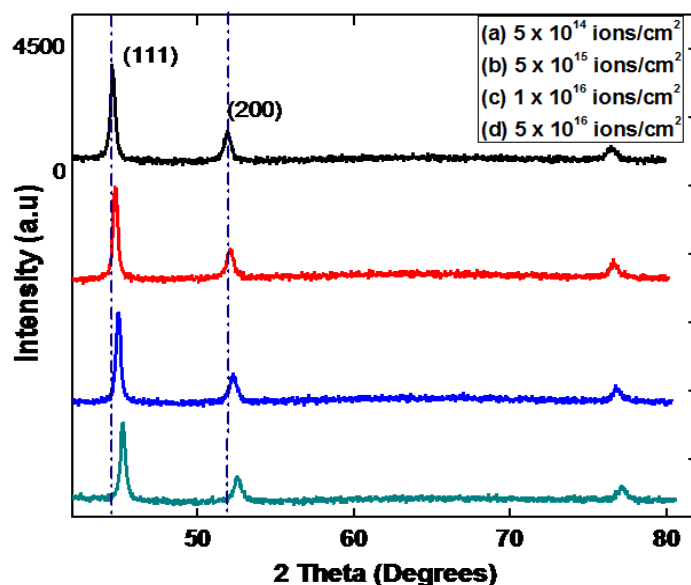


Figure 7: XRD spectra analysis of Ni-NWs network irradiated with 2.75 MeV of H^+ ions at various beam fluencies.

Structural information on 2.75 MeV H^+ ions irradiated Ni-NWs networks would also be supportive for elucidating the perceived changes in the conductivity of the materials. In order to verify the structure of the pristine and the irradiated Ni-NWs networks, the XRD measurements were conducted at R_T and presented in Fig.6. Un-irradiated sample is showing peaks of face centered cubic (fcc) structure of Ni-NWs [13].

After irradiation, a slight shifting in the value of 2θ of the diffraction peaks is seen in the XRD spectra when compared with the un-irradiated samples. The shifting in 2θ positions of the diffraction peaks might be owing to the presence of strain obtained; we presume due to surface defects or dislocations [14, 18]. We also observed that the peak intensities reduced as the ion beam fluence increases as seen Fig. 5. The XRD peaks are indicating reduction of intensity because defects are generated in the form of dislocations, grain boundaries and point defects. The defect clusters or pockets of amorphous regions are formed due to accumulation of these defects in the crystalline structure of NWs. The crystallinity of the material is degraded due to presence of defect clusters or amorphous regions [9, 14].

After the TEM and XRD analysis of Ni-NWs, four probe methods was employed to determined the conductivity mesh of the samples before and after irradiation. The electrical conductivity was observed to decrease at beam fluence $\sim 5 \times 10^{14}$ ions/cm² with respect to un-irradiated samples; meanwhile, after the fluence was increased to 5×10^{15} ions/cm², the electrical conductivity of Ni-NWs meshes was observed to be increased. This increment might be owing to the sputtered Ni atoms agglomerated nearby contact positions as well as local heating by the ion beam of Ni-NWs. Due to local heating of Ni-NWs, contact welding is initiated due to coalescence or fusion of NWs which lead to increase conductivity at this beam fluence slightly [10]. With the increment in beam fluence upto 1×10^{16} ions/cm², fusion or coalescence of the formed NWs was observed to be more visible as shown in Fig. 2. Cross and parallel junction formation between NWs due to H^+ ion irradiation induced fusion or coalescence of NWs is clearly seen in Fig. 2. The junction formations finally weld NWs and form a finely welded Ni-NWs mesh. At beam fluence of 5×10^{14} ions/cm², the conductivity of formulated Ni-NWs networks is increased to the order of 3.0. The observed increase of conductivity after irradiation is similar to carbon nanotubes (C-NTs) and silver nanowires (Ag-NWs) networks already demonstrated in our previous report [14, 19]. As fluence of H^+ ion is increased to $\sim 5 \times 10^{15}$ ions/cm², Ni-NWs network becomes highly conductive. Fused, welded junctions (cross and parallel) between Ni-NWs at irradiation fluence $\sim 5 \times 10^{15}$ ions/cm², were presented in TEM images of Fig. 3. At this beam fluence, the electrical conductivity of Ni-NWs mesh was recorded and observed to increase by 2.5 times referred with un-irradiated sample. The increase in the value of electrical conductivity might be due to the fusion or coalescence of NWs at junction positions which caused a decrease in resistance at contact points; hence a resistance free path is provided to electrons at junction locations. Further increase in ion beam fluence caused the NWs to melt, fuse and damage. TEM image of Fig. 4 is presenting this mutilation where these NWs were found to be melted, made thinned and cut into slices at high irradiation fluence 1×10^{16} ions/cm².

At high irradiation fluence of H^+ ions 5×10^{16} ions/cm², the NWs are damaged and conductivity is reduced. Variations of electrical conductivity in Ni-NWs are analyzed with irradiation fluence of H^+ ions, a plot of conductivity versus irradiation dose is presented.

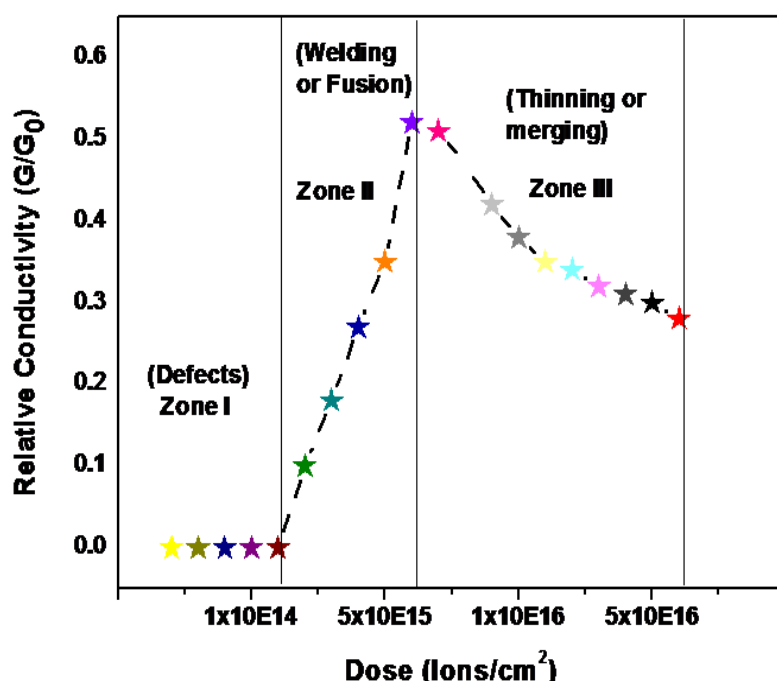


Figure 6: Electrical conductivity (relative i.e., G/G_0) of Ni-NWs meshes as a function of fluence of H^+ ions.

G is conductivity of irradiated sample and G_0 is the conductivity of un-irradiated sample whereas G/G_0 is relative conductivity of samples. At low irradiation fluence, conductivity is decreased slightly as indicated in “Zone I” of Fig.6. The obtained results are similar to Ag-NWs at different fluencies of Li^{3+} ions [14, 17]. A rise in conductivity value was clearly seen in Zone II which reaches a maximum value at beam fluencies between 5×10^{15} and 1×10^{16} ions/cm² as shown in Fig.6. The observed increase in conductivity might be due to reduction in defects which was produced at low irradiation fluencies; caused as results of local heating induced fusion or coalescence of NWs at high irradiation fluence. A further decrease in the conductivity with further increase in beam fluence that might be due to thinning, slicing and melting of NWs was observed in Zone III. The observed changes in value of conductivity of Ni-NWs with H^+ ions irradiation fluence can be fully understood by calculating H^+ ion irradiation induced damage in Ni layer using Stopping and Range of Ions in Matter (SRIM) simulation program. Fig. 7 (a-b) represents the plots of ions tracks and impact events.

The red colored dots in Fig. 7 (a) is representing a vacancy induced due to impact of H^+ ion with a lattice of Ni layer. Similarly, figure 7 (b) shows the collision events.

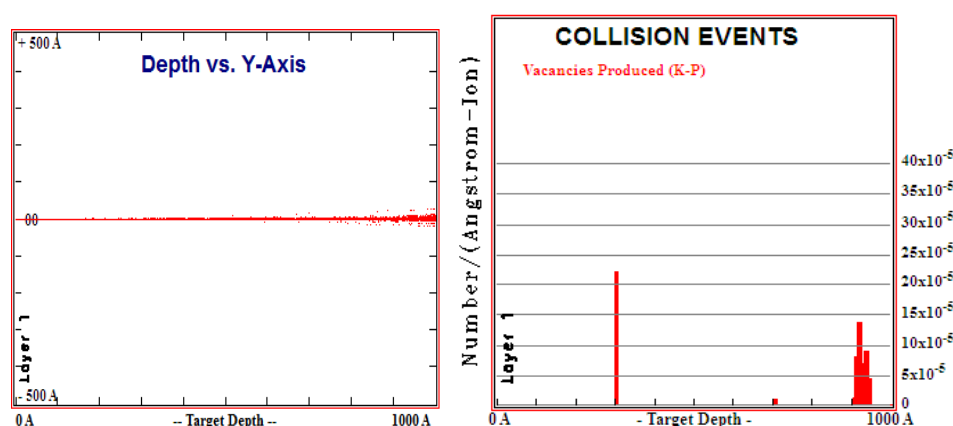


Figure 7: SRIM simulation results (a) Path of H^+ ions on Y-axis (b) Collision impacts in Ni layer

Table 1 shows simulation results for interaction of H^+ ion with Ni layer. Simulation was performed for loss of energy of H^+ ions, total damage and recoils at 2.75 MeV. Incident angle was opted to be 0° . The term ionization represents loss of energy to target electrons. The direct transfer of energy from H^+ ion to Ni layer is

represented in data column of ions whereas transfer of energy due to recoil atoms is represented in data column of recoils.

Simulation results are showing that diffusion of H^+ ions into Ni layer produced defects in lattice. These defects are produced in Ni-NWs in form of vacancies and caused to reduce in conductivity of NWs. After initiation of coalescence or fusion of NWs, contact resistance of NWs is reduced, path length is increased and consequently conductivity is increased. XRD and simulation results collectively represents that both phenomena such as coalescence of NWs due to heat and production of lattice defects are occurring concurrently within NWs after exposure to H^+ ions. However, induction of localize heat is dominant process as compared to creation of defects. If the beam fluence is low, coalescence process of NWs is dominant and increased path length; consequently, conductivity is increased. In case of high irradiation fluence 1×10^{16} ions/cm², both localize heating effect and generations of defects are appearing in the structure concurrently. Besides, less path length is occurred after exposure of NWs to high fluences of H^+ ions which is due to cutting and slicing of NWs; consequently, reduces conductivity. On the basis of present experimental findings and previous experiments, it is found that changes of electrical conductivity of Ni-NWs have been occurred which could be tuned for numerous nanotechnology applications. Fig. 8 (a-c) shows a schematic representation of whole experimental steps starting from un-irradiated network (a) to formation of various types of interconnections between NWs (b) and finally damaging of NWs at high beam fluence (c).

Table 1: Simulation of H^+ ions interacting with Ni layer.

Total Number of Vacancies/Ion	% of Energy Loss (Ion)		% of Energy Loss (Recoil)	
	Ionization	Phonons	Ionization	Phonons
21	99.74	0.01	0.06	0.18

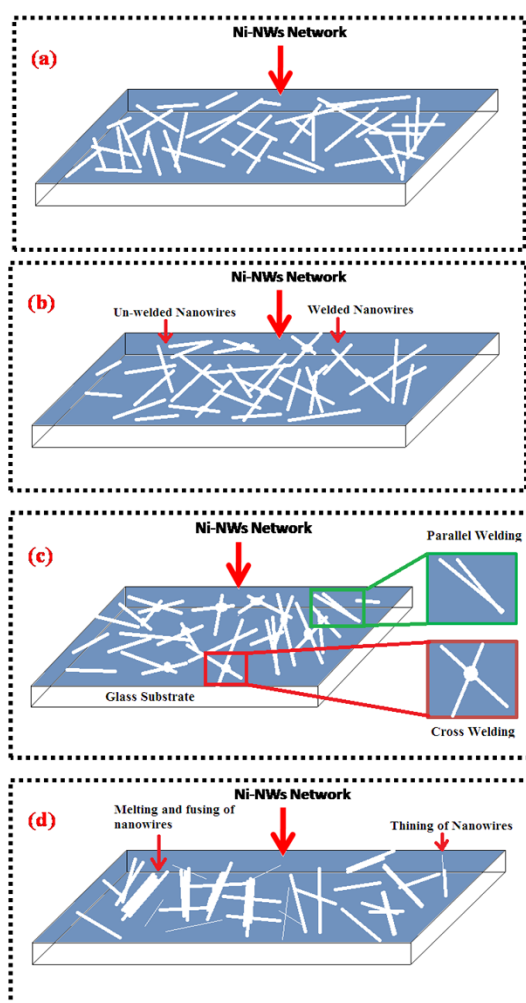


Fig. 8: Ni-NWs mesh (a) without irradiation. Various stages after exposure to radiations (b) welding initiation (c) junction formation in cross and parallel shapes (d) Melting, fusing and thinning of NWs.

IV. CONCLUSION

In summary, welding of NWs is obtained by exposure to beams of energetic H^+ ions. Coalescence will cause the reduction of wire-wire resistance on joints and due to which an improvement in electrical conductivity is found. This improvement of electrical conductivity is observed in NWs at low doses. After irradiating at high beam fluencies of H^+ ions, NWs was found to be sliced, broken and melted. The present approach is superb for fabrication of highly conductive NWs networks. This study is useful in many current nanotechnology applications where high electrical conductivity is required.

ACKNOWLEDGEMENT

Financial support of HEC, TWAS-UNISA-iThemba LABS-National Research Foundation, JIRCANDE is greatly acknowledged.

REFERENCES

- [1]. S. De, T. M. Higgins, P.E. Lyons, E.M. Doherty, P.N. Nirmalraj, W.J. Blau, J.J. Boland, J.N. Coleman, ACS nano. 3 (2009) 1767.
- [2]. J.Y. Lee, S.T. Connor, Y. Cui, P. Peumans, Nano Lett. 8 (2008) 689.
- [3]. H. Wu, D. Kong, Z. Ruan, P.C. Hsu, S. Wang, Z. Yu, T.J. Carney, L. Hu, S. Fan, Y. Cui, Nature nanotech. 8 (2013) 421.
- [4]. Y. Lu, J.Y. Huang, C. Wang, S. Sun, J. Lou, Nat. Nanotech. 5 (2010) 218.
- [5]. J. A. Spechler, C.B. Arnold, Appl. Phys. A. 108 (2012) 25.
- [6]. H. Tohmyoh, S. Fukui, J. Nanoparticle Res. 14 (2012) 1.
- [7]. P. Lee, J. Lee, H. Lee, J. Yeo, S. Hong, K.H. Nam, D. Lee, S.S. Lee, S.H. Ko, Adv. Mat. 24 (2012) 3326.
- [8]. A. Ishaq, L. Yan, D. Zhu, Nucl. Instrum. Methods Phys. Res. B. 267 (2009) 1779.
- [9]. A. Ishaq, L. Yan, G. Husnain, B. Lu, M. Arshad, A. Khalid, Nano. 6 (2011) 357.
- [10]. H. Shehla, A. Ishaq, Y. Khan, I. Javed, R. Saira, N. Shahzad, , M. Maaza. Ion beam irradiation-induced nanowelding of Ag Nanowires. Micro and nano letters, 11(1) (2016) 34-37.
- [11]. Honey S, Naseem S, Ishaq A, Maaza M, Bhatti M T, Wan D. Large scale silver nanowires network fabricated by MeV hydrogen (H^+) ion beam irradiation. Chin. Phys. B. 25 (4) (2016) 046100.
- [12]. Honey S, Naseem S, Ishaq A, Maaza M. Bhatti M T, Madhuku M. Interconnections between Ag-NWs build by argon ions beam irradiation. J Nanomater. Mol. Nanotechnol. 6(2) (2017).
- [13]. Honey S., Ishaq A. Madhuku M., Naseem S., Maaza M., Kennedy J. V. Nickel nanowires mesh fabricated by ion beam irradiation-induced nanoscale welding for transparent conducting electrodes. Material Research Express. 4 (2017) 075042.
- [14]. B. Bushra, H. Shehla, M. Madhuku, A. Ishaq, R. Khan, M. Arshad, K. Alamgir, S. Naseem, M. Maaza. MeV Carbon Ion Irradiation-Induced changes in the electrical conductivity of Silver Nanowire networks. Current Applied Physics 15 (2015), 642.
- [15]. I. Ahmad, W. Akram, G. Husnain, Y. Long, Z. Xingtai, Curr.Nanosci. 7 (2011) 790.
- [16]. A.V. Krashennikov, K. Nordlund, J. Appl. Phys. 107 (2010) 071301.
- [17]. Chang Fu Dee, Ishaq Ahmad, Yan Long, Zhou Xingtai, M. M. Salleh, B. Y. Majlis. Contact welding study of carbon nanotube with ZnO nanowire. Physica E 43 (2011) 1857-1862.
- [18]. Pallavi Rana and R. P. Chauhan. Physica B 451 (2014), 26-33.
- [19]. A. Sharma, K.D. Verma, M. Varshney, D. Singh, M. Singh, K. Asokan, R. Kumar. Rad. Eff. & Def. Sol: Incorporating Plas. Sci. & Plas. Technol. 165 (2010) 930.